Rheological Properties of a Two Phase Lipid Monolayer at the Air/Water Interface: Effect of the Composition of the Mixture

N. Wilke,* F. Vega Mercado, and B. Maggio

CIQUIBIC, Dpto. de Química Biológica, Facultad de Ciencias Químicas, Universidad Nacional de Córdoba, Pabellón Argentina, Ciudad Universitaria, X5000HUA Córdoba

Many biologically relevant monolayers show coexistence of discrete domains of a long-range ordered condensed phase dispersed in a continuous, disordered, liquid-expanded phase. In this work, we determined the viscous and elastic components of the compressibility modulus and the shear viscosity of monolayers exhibiting phase coexistence with the aim at elucidating the contribution of each phase to the observed monolayer mechanical properties. To this purpose, mixed monolayers with different proportions of distearoylphosphatidylcholine (DSPC) and dimyristoylphosphatidylcholine (DMPC) were prepared and their rheological properties were analyzed. The relationship between the phase diagram of the mixture at 10 mN m^{-1} and the rheological properties was studied. We found that the monolayer shear viscosity is highly dependent on the presence of domains and on the domain density. In turn, the monolayer compressibility is only influenced by the presence of domains for high domain densities. For monolayers that look homogeneous on the micrometer scale (DSPC amount lower that 23 mol %), all the analyzed rheological properties remain similar to those observed for pure DMPC monolayers, indicating that in this proportion range the DSPC molecules contribute as DMPC to the surface rheology in spite of having hydrocarbon chains four carbons longer.

1. Introduction

Contrary to the Singer and Nicolson fluid mosaic model,[1] most natural membranes show phase coexistence, normally characterized by segregated domains in a more fluid environment. It is expected (and has already been demostrated in several systems) that the presence of the domains influences not only the local but also the macroscopic rheological properties of the membrane. For example, the diffusion of molecules residing either within domains or in the continuum phase is decreased in the presence of domains.[2−7]

In turn, the rheological properties of the membrane influence important biological phenomena, such as the fusion of vesicles, the breakdown of foams and emulsions, the opening of transitory pores, and the lateral diffusion of the components in membranes, which is a factor that determines, among others, the velocity of biochemical reaction−diffusion processes[8] and thus the function of cells.[9] The understanding of factors that define the mechanical properties of membranes, being complex two-dimensional fluids, is an active research area that has not yet been completely deciphered. The domains, which can reach to tens of micrometers,[10,11] provide an inhomogeneous scenario, not only related to rheological properties but also to electrostatics. The electrostatic field generated by the domains can attract or repel the diffusing components thus influencing its lateral motion.[5,12]

Lipid monomolecular layers at the air−water interface provide a useful model of biointerfaces because their density can be varied over the entire range from the gaseous up to the liquid condensed state. Besides, surface rheology can be studied by a variety of experimental techniques in which the environment of the diffusing species can be controlled and also varied in a controlled manner. It has been observed that the shear viscosity of monolayers and bilayers is of the same order of magnitude[3,7] and the diffusion of species inserted in both film structures are hindered by the presence of domains.[4−6,13−15] Langmuir lipid monolayers have provided fundamental knowledge on the structural dynamics of biomembranes as suitable model systems that can also shed light

*To whom correspondence should be addressed. Mailing address: CIQUIBIC, Dpto. de Química Biológica, Facultad de Ciencias Químicas, Universidad Nacional de Córdoba, Pabellón Argentina, Ciudad Universitaria, X5000HUA Córdoba. E-mail: wilke@mail.fcq.unc.edu.ar. Telephone/Fax: +54-351-4334171.

(1) Singer, S. J.; Nicolson, G. L. The fluid mosaic model of the structure of cell membranes. *Science* **1972**, *175* (23), 720−731.

(2) Ding, J.; Warriner, H. E.; Zasadzinski, J. A. Viscosity of two-dimensional suspensions. *Phys. Rev. Lett.* **2002**, *88* (16), 168102.

(3) Cicuta, P.; Keller, S. L.; Veatch, S. L. Diffusion of liquid domains in lipid bilayer membranes. *J. Phys. Chem. B* **2007**, *111* (13), 3328−3331.

(4) Saxton, M. J. Lateral diffusion in an archipelago. Dependence on tracer size. *Biophys. J.* **1993**, *64* (4), 1053−1062.

(5) Forstner, M. B.; Martin, D. S.; Ruckerl, F.; Kas, J. A.; Selle, C. Attractive membrane domains control lateral diffusion. *Phys. Rev. E: Stat., Nonlinear, Soft Matter Phys.* **2008**, *77* (5 Pt 1), 051906.

(6) Selle, C.; Ruckerl, F.; Martin, D.; Forstner, M. B.; Kas, J. A. Measurement of diffusion in Langmuir monolayers by sinlge-particle tracking. *Phys. Chem. Chem. Phys.* **2004**, *6*, 5535−5542.

(7) Wilke, N.; Maggio, B. The influence of domain crowding on the lateral diffusion of ceramide-enriched domains in a sphingomyelin monolayer. *J. Phys. Chem. B* **2009**, *113* (38), 12844−12851.

(8) Thompson, T. E.; Sankaram, M. B.; Biltonen, R. L.; Marsh, D.; Vaz, W. L. Effects of domain structure on in-plane reactions and interactions. *Mol. Membr. Biol.* **1995**, *12* (1), 157−162.

(9) Bhalla, U. S.; Iyengar, R. Emergent properties of networks of biological signaling pathways. *Science* **1999**, *283* (5400), 381−387.

(10) Veatch, S. L.; Keller, S. L. Organization in lipid membranes containing cholesterol. *Phys. Rev. Lett.* **2002**, *89* (26), 268101.

(11) Stottrup, B. L.; Stevens, D. S.; Keller, S. L. Miscibility of ternary mixtures of phospholipids and cholesterol in monolayers, and application to bilayer systems. *Biophys. J.* **2005**, *88* (1), 269−276.

(12) Nassoy, P.; Birch, W. R.; Andelman, D.; Rondelez, F. Hydrodynamic mapping of two-dimensional electric fields in monolayers. *Phys. Rev. Lett.* **1996**, *76* (3), 455−458.

(13) Saxton, M. J.; Jacobson, K. Single-particle tracking: applications to membrane dynamics. *Annu. Rev. Biophys. Biomol. Struct.* **1997**, *26*, 373−399.

(14) Tang, Q.; Edidin, M. Vesicle trafficking and cell surface membrane patchiness. *Biophys. J.* **2001**, *81* (1), 196−203.

(15) Kusumi, A.; Sako, Y.; Yamamoto, M. Confined lateral diffusion of membrane receptors as studied by single particle tracking (nanovid microscopy). Effects of calcium-induced differentiation in cultured epithelial cells. *Biophys. J.* **1993**, *65* (5), 2021−2040.

on the influence of domains on the mechanical properties of biointerfaces[16] such as bidimensional fluids.

Monolayers and bilayers of the binary mixture of dimyristoyl-phosphatidylcholine (DMPC) and distearoylphosphatidylcholine (DSPC) have been widely studied.[17−23] The lateral pressure−molecular area compression isotherm of DMPC at 23 °C shows a behavior expected for a liquid-expanded film while DSPC forms liquid-condensed films with a solid−solid phase transition at 25 mN m^{-1}.[24] Mixed DSPC/DMPC monolayers and bilayers show nonideal behavior.[17−23]

In this work we determined some properties that describe the mechanical behavior of monolayers of different DSPC/DMPC proportions. We measured the diffusion coefficient of species inserted in the monolayer, from where the shear viscosity was estimated. Besides, the isotherm compression modulus was obtained from the lateral pressure-average molecular area isotherm. Since this parameter contains both the elastic and the viscous component of the complex compression modulus, oscillatory compression−expansion cycles were also performed and both components were obtained separately. In this manner, we could analyze the effect of the proportion of DSPC on the mechanical properties of these monolayers in the one-phase and in the two-phase coexistence regions. This allows investigating some of the possible reasons for the observed monolayer mechanical properties.

2. Experimental Section

2.1. Materials. Distearoylphosphatidylcholine (DSPC), dimyristoylphosphatidylcholine (DMPC), and the lipophilic fluorescent probe L-α-phosphatidylethanolamine-*N*-(lissamine rhodamine B sulfonyl) ammonium salt (chicken egg, trans-phosphatidylated) were purchased from Avanti Polar Lipids (Alabaster, AL). Micrometer-sized beads (0.9 μm diameter, car-boxylate-modified beads) were purchased from SIGMA. We selected these modified beads to minimize the bead−bead and bead−domain interaction previously observed for polystyrene latex beads.[12] The beads were cleaned by successive centrifugation followed by remotion of the supernatant; the pellet was resuspended in MQ water. This procedure was repeated 10 times. Solvents and chemicals were of the highest commercial purity available. The water used for the subphase was from a Milli-Q system (Millipore, 18 MΩ). Lipid monolayers were prepared and characterized in different Langmuir film balances with isometric compression, on NaCl 0.45 M subphases at (23 ± 1) °C.

2.2. Methods. *2.2.1. Fluorescence Microscopy (FM) and Phase Contrast Microscopy Experiments.* For the FM experiments, the fluorescent probe was incorporated in the lipid solution before spreading (1 mol %). After spreading the lipid layer, the subphase level was reduced to a thickness of about 3 mm to minimize convection. Besides, a glass mask with lateral slits extending through the film into the subphase was used to restrict lateral monolayer flow under the field being observed. The Langmuir film balance (microthrough, Kibron, Helsinki, Finland) was placed on the stage of an inverted fluorescence microscope (Axiovert 200, Carl Zeiss, Oberkochen, Germany) with a 40× or a 20× objective. Images were registered by a CCD video camera AxioCam HRc (Carl Zeiss, Oberkochen, Germany) commanded through the Axiovision 3.1 software of the Zeiss microscope. For the analysis of the micrometer-sized bead motion, we recorded images of the monolayer without fluorescent probe using phase contrast microscopy and the same setup as for the FM experiments. The previously cleaned beads were resuspended in water, forming a concentrated clean bead solution (~10^{10} beads/mL). A small volume (lower than 5% of the final volume to avoid phase separation) of this concentrated bead solution was added to the lipid mixture previously dissolved in chloroform/methanol (2:1), and this mixture was spread at the air−water interface. The final bead density was normally about 1 bead in 2000−2500 μm^2.

2.2.2. Diffusion Coefficient of Beads and Domains. The calculation of the diffusion coefficient of domains D_D and of micrometer-sized beads D_B was performed as explained in ref 7. Briefly, images of the surface of the monolayer were recorded for 50 s (1 frame/s). Then the relative positions of domains or beads selected in pairs were followed through the 50 frames. The mean square displacement of a domain or bead relative to another (MSD$_{rel}$) was calculated for different time lapses between frames (δt) as MSD$_{rel}$ = $\langle |\vec{X}_{rel}^{t+\delta t} - \vec{X}_{rel}^{t}|^2 \rangle$. MSD$_{rel}$ was plotted as a function of δt for each experimental condition. If the domains or beads in the selected pair are in the same environment, the drift of each particle should be similar. Additionally, if they are of approximately the same size, the diffusion coefficient would be the same. In these conditions, MSD$_{rel}$ = $8D\delta t$.[7,25] We only analyzed the motion of small domains (7−16 μm^2); since the data dispersion is larger than the theoretical dependence of D_D with the domain size at this size range (see Figure 7A and ref 7), D_D for all the analyzed domains was averaged without taking into account their size.

The trajectories of beads too close to each other (less than 10 μm) were discarded for the D_B determination, since capillarity effects between each particle could be influencing their motion. All the analyzed beads were at the interface and not in the subphase, since no beads were found at higher focuses and since the tracked beads were in the focus during all of the recording (their motion was only two-dimensional). In the case of mono-layers with 30 and 40 mol % DSPC (two-phase systems), we performed control experiments with fluorescent probes to rule out sticking of the beads to the domain border and/or coupling of the bead motion with the motion of the domains. Monolayers with amounts of DSPC higher than 40 mol % were not analyzed using the tracking of beads at the interface. At least 40 trajectories of pairs of domains or beads were tracked in each independent experiment for a given DSPC/DMPC proportion.

At high domain density (in our case DSPC content higher than 45 mol %), the domain motion is coupled to their closest neighbor domains. Therefore, the relative MSD of a particular domain was referred to domains at increasing distances. In some experiments, the resultant diffusion coefficient values were higher the higher the distance between the pair of domains, reaching a plateau for a distance between the tracked domains of about 200 μm. The plateau value was three times higher than the value for the closest

(16) Brockman, H. L. Lipid monolayers: why use half a membrane to char-acterize protein-membrane interactions? *Curr. Opin. Struct. Biol.* **1999**, *9*, 438−443.

(17) Kubo, I.; Adachi, A.; Maeda, H.; Seki, A. Phosphatidylcholine monolayers observed with Brewster angle microscopy and pressure-area isotherms. *Thin Solid Films* **2001**, *393*, 80−85.

(18) Sugar, I. P.; Thompson, T. E.; Biltonen, R. L. Monte Carlo simulation of two-component bilayers: DMPC/DSPC mixtures. *Biophys. J.* **1999**, *76* (4), 2099−2110.

(19) Leidy, C.; Wolkers, W. F.; Jorgensen, K.; Mouritsen, O. G.; Crowe, J. H. Lateral organization and domain formation in a two-component lipid membrane system. *Biophys. J.* **2001**, *80* (4), 1819−1828.

(20) Arnold, A.; Cloutier, I.; Ritcey, A. M.; Auger, M. Temperature and pressure dependent growth and morphology of DMPC/DSPC domains studied by Brewster angle microscopy. *Chem. Phys. Lipids* **2005**, *133* (2), 165−179.

(21) van Dijck, P. W.; Kaper, A. J.; Oonk, H. A.; de, G. J. Miscibility properties of binary phosphatidylcholine mixtures. A calorimetric study. *Biochim. Biophys. Acta* **1977**, *470* (1), 58−69.

(22) Mabrey, S.; Sturtevant, J. M. Investigation of phase transitions of lipids and lipid mixtures by sensitivity differential scanning calorimetry. *Proc. Natl. Acad. Sci. U.S.A.* **1976**, *73* (11), 3862−3866.

(23) Shimshick, E. J.; McConnell, H. M. Lateral phase separation in phospho-lipid membranes. *Biochemistry* **1973**, *12* (12), 2351−2360.

(24) Phillips, M. C. The physiscal state of phospholipid and cholesterol in monolayers, bilayers, and membranes. In *Progress in Surface and Membrane Science*; Danielli, J. F., Rosenberg, M. D., Cadenhead, D. A., Eds.; Academic Press: New York, 1972; pp 139−221.

(25) Sickert, M.; Rondelez, F.; Stone, H. A. Single-particle Brownian dynamics for characterizing the rheology of fluid Langmuir monolayer. *Europhys. Lett.* **2007**, *79*, 66005−66011.

pair of domains. For this reason, domain diffusion coefficient was also calculated using single-domain tracking. This could be performed, since in our experiments the drift in the domain movement was linear with time and homogeneous for all domains in the images. Taking this into account, an average convection was estimated from the motion of all the tracked domains in the images. This average convection was subtracted from a particular domain motion, and the resulting MSD was used for the determination of the diffusion coefficient value. The values obtained with this approach were the same as those we obtained for a pair of domains far from each other. Convections nonlinear with time ($R^2 < 0.98$) or not homogeneous in the images (tolerance 5%) were not considered for the analysis.

2.2.3. Brewster Angle Microscopy (BAM) Experiments. The condensed area percent was calculated using FM and BAM. In BAM, no fluorescent probe addition is necessary. These experiments were performed to ensure that the probe was not altering the phase area percent, since the distribution of the fluorescent probe may not be homogeneous between phases. We used an EP[3] Imaging ellipsometer (Accurion, Goettingen, Germany) with a 20× objective, and the monolayer was spread in a Langmuir film balance (model 102M, Nima Technology Ltd., Coventry, England).

2.2.4. Dilatational Rheology Experiments. These experiments were performed using a Langmuir film balance (KSV minithrough, KSV Instruments, Ltd., Helsinki, Finland), as described in detail by Cicuta and Terentjev.[26] Briefly, the Langmuir film of the lipid mixture under study was compressed isometrically up to the desired lateral pressure. Then sinusoidal area perturbations by compression−expansion were performed while measuring both the surface pressure and the phase shift between the tension and the surface area signals.

Since the deformation created by the moving barrier is uniaxial, it is a superposition of well-defined dilatation and shear. Therefore, taking into account that the interfacial tension is a tensorial quantity, the measured values depend on the direction of the length along which the stress acts.[27] For that reason, if two Wilhelmy plates are placed in orthogonal positions, the following equations describe the response of the system:[26]

$$|E^* + G^*| = A_0 \frac{\Delta \pi_{\parallel}}{\Delta A} \qquad (1)$$

$$|E^* - G^*| = A_0 \frac{\Delta \pi_{\perp}}{\Delta A} \qquad (2)$$

where E^* is the complex dilatational compressibility, G^* is the complex shear modulus and $\Delta \pi_{\parallel}$ and $\Delta \pi_{\perp}$ are the lateral pressure fluctuation registered by the plates placed parallel and perpendicular to the barriers, respectively. The loss and storage component of each complex modulus can be computed knowing the retardation angle. For a detailed description of the technique, readers are referred to ref 26.

In all the cases analyzed in this work, both Wilhelmy plates gave, within errors, the same response which is in agreement with the low shear viscosity derived from the domain and bead diffusion coefficient (see Results section).

2.2.5. Electrostatic Field Application to the Lipid Monolayer. The experimental setup for applying an electrostatic field to the lipid monolayer was the same as that used previously.[7,28,29] Briefly, a metal wire is held at 200 μm above the subphase.

(26) Cicuta, P.; Terentjev, E. M. Viscoelasticity of a protein monolayer from anisotropic surface pressure measurements. *Eur. Phys. J. E* **2005**, *16*, 147−158.

(27) Petkov, J. T.; Gurkov, T. D. Dilatational and shear elasticity of gel-like protein layers on air/water interface. *Langmuir* **2000**, *16*, 3703−3711.

(28) Wilke, N.; Dassie, S. A.; Leiva, E. P.; Maggio, B. Externally applied electric fields on immiscible lipid monolayers: repulsion between condensed domains precludes domain migration. *Langmuir* **2006**, *22* (23), 9664−9670.

(29) Wilke, N.; Maggio, B. Effect of externally applied electrostatic fields on the surface topography of ceramide-enriched domains in mixed monolayers with sphingomyelin. *Biophys. Chem.* **2006**, *122* (1), 36−42.
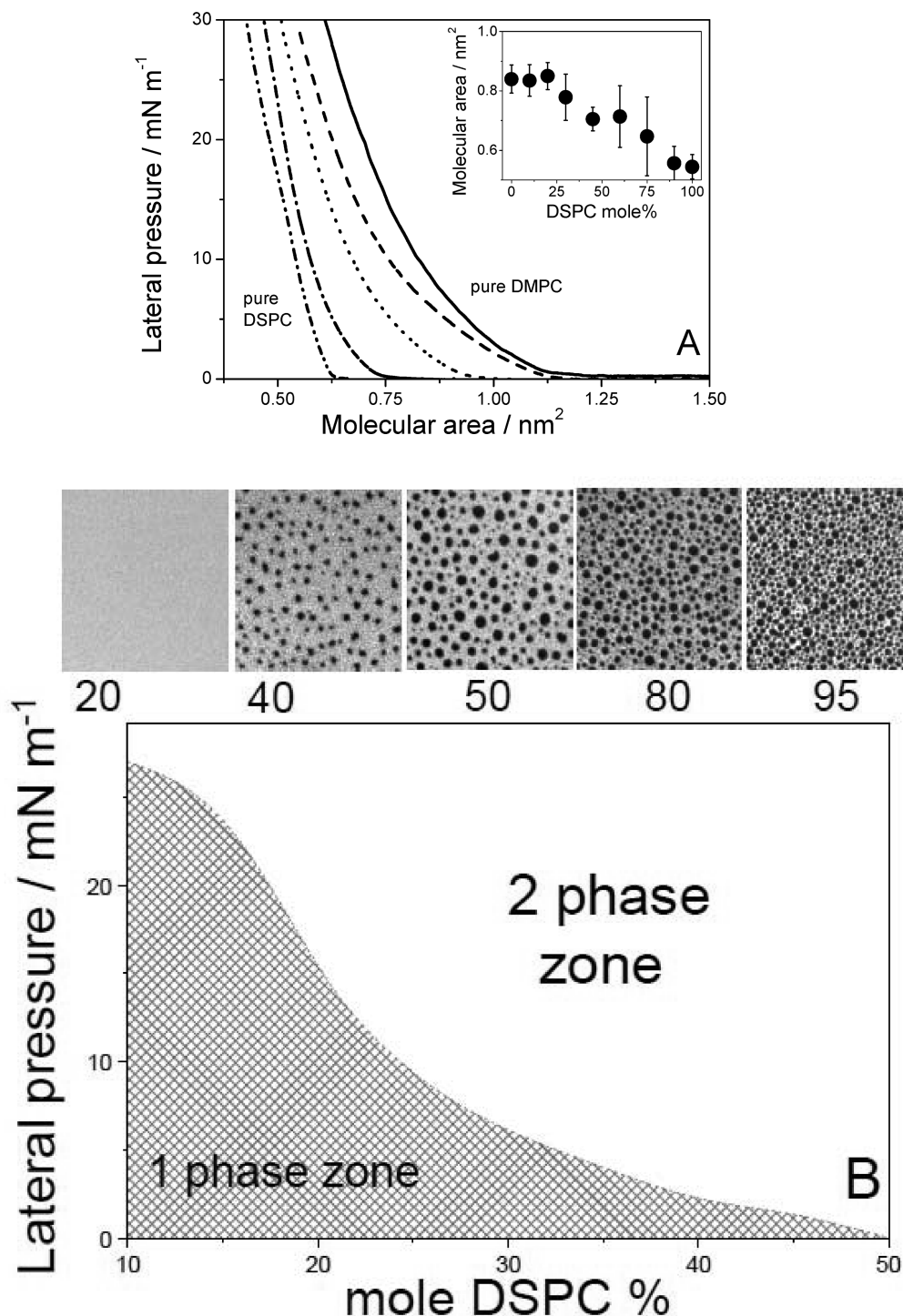
A second electrode is placed in the subphase, and a potential difference is applied between the electrodes. The upper electrode was charged by applying potentials of up to 300 V with respect to the subphase electrode. If the dipole density of the domains is different from the dipole density of the continuous phase, an inhomogeneous electric field will generate a net force on the domains. In the system under study, the dipole density inside the domains is higher than that in the continuous phase (the surface potential is 150 mV higher, data not shown). Therefore, a positive potential leads to domain migration away from the zone under the electrode above the subphase. When the desired domain array was achieved, the field was turned off and images of the surface of the DSPC/DMPC monolayer were recorded.

3. Results

Pure DMPC and DSPC compression isotherms have been described previously in several reports. At room temperature, DMPC shows a behavior expected for a liquid-expanded film and DSPC forms liquid-condensed films with a solid−solid phase transition at 25 mN m^{-1}.[24] Mixed DSPC/DMPC monolayers and bilayers show nonideal behavior.[17−20] Figure 1A shows the lateral pressure−molecular area compression isotherms for pure lipids and some of their mixtures on NaCl 0.45 M solutions at 23 °C. The inset shows the average molecular area as a function of the DSPC mol % at 10 mN m^{-1}. The nonideal behavior is clear in this plot; the average molecular area remains constant for DSPC mol % lower than 23 mol %, and for higher DSPC amounts it decreases.

This section is organized in three subsections: We first describe the bidimensional phase diagram for the DMPC/DSPC mixture and the distribution of domains at different DMPC/DSPC proportions (section 3.1). In section 3.2, the dilatational monolayer compressibility for different lipid proportions in the mixture is analyzed, and finally, in Section 3.3, the Brownian motion of domains and of microbeads at the interface is determined.

3.1. Phase Diagram for the DSPC/DMPC Mixture. Figure 1B shows the lateral pressure and composition region were the mixed monolayers show two-phase coexistence, with liquid-condensed macroscopic domains dispersed in a liquid-expanded continuous phase. In the same figure, representative micrographs at 10 mN m^{-1} are also displayed. We will now focus on the properties of mixed monolayers at 10 mN m^{-1}; this lateral pressure was chosen because it is away from the lift-off of the lateral pressure−molecular area compression isotherm and also from the collapse pressure for DMPC or the rearrangement pressure point for DSPC ("kink" at 25 mN m^{-1} (ref 24)). At 10 mN m^{-1}, the monolayer is homogeneous on the micrometer scale (0.25 μm^2) for DSPC amounts lower than 23 mol %. For higher DSPC proportions, segregated domains of a phase where the fluorescent probe is less soluble appear. For 23 < DSPC mol % < 65, the amount of domains increases as the DSPC proportion increases without perceptible changes of the average domain size (22 ± 9 μm^2). For mixed monolayers with DSPC content above 65 mol %, the amount of domains reaches a plateau. This is evident in Figure 2A, where the percent of the total monolayer area occupied by domains is plotted as a function of the mol % of DSPC. In this figure, the dashed line corresponds to the theoretical curve for a system with the same phases in coexistence at proportions from 23 to 100 mol % DSPC. The calculation of this curve was performed considering that the DSPC/DMPC ratio in the continuous phase remains constant in all of this composition range (from 23 to 100 mol % DSPC) at a value of 23/77 = 0.3 (30 mol % DSPC with respect to the total moles in this phase). Besides, taking into account the constancy of the average molecular area for compositions from 0 to 23 DSPC mol % (see inset in

Figure 1. (A) Representative compression isotherms for DSPC/DMPC mixed monolayers: (from right to left) 0, 25, 50, 75, and 100 mol % DSPC. Inset: Average molecular area at 10 mN m^{-1} as a function of the DSPC mol % in the mixture. (B) Phase diagram (lateral pressure versus composition) for mixed DSPC/DMPC monolayers. The one phase−two phase limit was determined by fluorescence microscopy experiments. The images are representative micrographs at 10 mN m^{-1} and for the indicated DSPC mol %. Images size: 100 μm × 100 μm.

Figure 1), we assumed that the average molecular area of the molecules in the continuous phase is similar to the value for pure DMPC molecules (0.8 nm^2). The domains were considered as composed of pure DSPC molecules. This assumption was based on the observation that monolayers composed of only 3 mol % DMPC show phase coexistence (data not shown), from what it follows that domains are almost pure DSPC (at least with less than 3 mol % DMPC). At high domain area percents, the probe becomes concentrated in the more fluid lipid phase. Therefore, control experiments were performed without probe, using BAM

microscopy (open symbols in Figure 2A). Figure 2B shows the radial domain distribution for different DSPC proportions. For 30 mol % of DSPC there is no significant most probable domain distance which means that the domains are in a disordered lattice. For a higher amount of DSPC (see curve labeled "40%"), domain−domain repulsions restrict them in a long-term order as already described for other lipid mixtures.[30] For monolayers

---

(30) McConnell, H. M. Structures and transitions in lipid monolayers at the air-water interface. *Annu. Rev. Phys. Chem.* **1991**, *42*, 171−195.
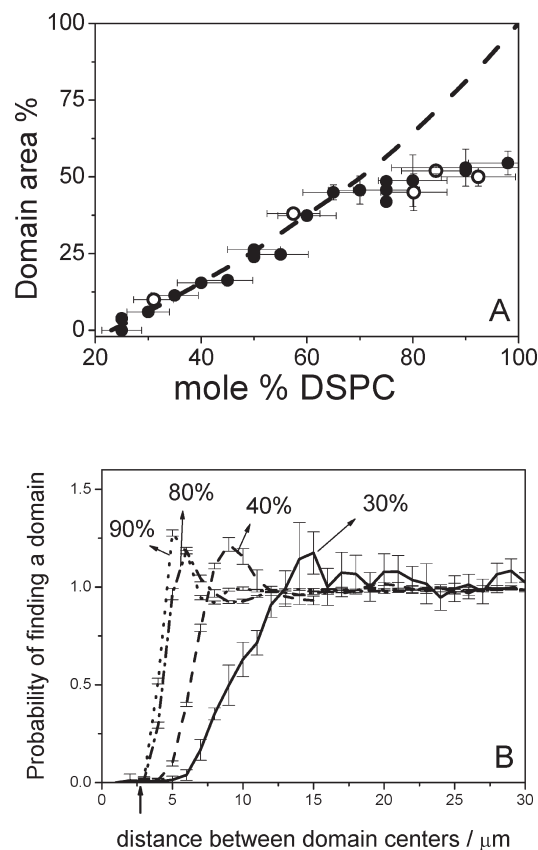
Figure 2. (A) Percent of the total monolayer area occupied by domains as a function of the monolayer composition for mixed DSPC/DMPC monolayers determined by fluorescence microscopy experiments (filled symbols) or by Brewster angle microscopy experiments (open symbols). The line corresponds to the theoretical curve considering two phases in coexistence, a continuous phase with a DSPC/DMPC proportion of 30 mol % of DSPC and an average molecular area of 0.8 nm² and domains of pure DSPC with an average molecular area of 0.5 nm² (see text). (B) Radial distribution of domains for monolayers with 30, 40, 80, and 90 mol % DSPC (from right to left). The arrow in the abscissa indicates the average domain size for all the proportions shown ($22 \pm 9 \, \mu m^2$).

with DSPC mol % higher than 40, the amount of domains also increases and the most probable nearest neighbor distance decreases as a consequence. However, this value reaches a plateau with DSPC mol % approaching 100%. In Figure 2B, the arrow on the abscissa indicates the average domain radius. No percolation point is observed for any DSPC/DMPC proportion at 10 mN m⁻¹.

Figure 2 indicates that, for a 65% mole percentage of DSPC or higher, the domains become highly ordered, forming a closely packed array where each domain has an average available area of about 35 μm². The percentage of condensed area experimentally found for DSPC proportions above 65 mol % is lower than the theoretical prediction for two phases in coexistence, with constant composition and average molecular area, which would appear to violate the lever rule. This deviation could be explained by considering that, for high DSPC proportions, the amount of molecules close to the domain boundaries is no longer negligible (it represents about 1% of the molecules considering that only the first ring of molecules are affected by the domain border), and the presence of the phase boundary is influencing the free energy of each phase, and thus the phase diagram. The experimental results indicate that either the average molecular area or the composition

of the phases changes. In the first case, the expanded phase should further expand while the condensed one would decrease its area. In the second case, the continuum phase should become enriched in DSPC. It would be unexpected that the average molecular area of the expanded phase should further increase when the proportion of DSPC in the mixture increases. However, at this stage of our study, we have no direct evidence for discarding either of the possibilities above. On the contrary, for DSPC mol % in the range 23−65%, changes in the DSPC proportion influence the amount of domains, without changing the properties in each phase.

In the following sections, the rheological properties of mixed monolayers of different DSPC/DMPC proportions at 10 mN m⁻¹ are analyzed.

3.2. Dilatational Compression Modulus. Figure 3A shows the isotherm compression modulus ($\varepsilon = -A(\partial \pi / \partial A)|_T$) calculated at 10 mN m⁻¹ for mixed monolayers at different DSPC/DMPC proportions (circles) and the curve expected for an ideal mixture[31] (line). The monolayer compressibility highly deviates from the ideal behavior in both the two-phase region and in the homogeneous region (DSPC mol % lower than 23%). For DSPC/DMPC monolayers with DSPC proportions lower than 60 mol %, values of ε similar to that obtained for pure DMPC monolayers are observed. Higher amounts of DSPC lead to abrupt increases of the monolayer compression modulus.

For quasi-static compression velocity, ε is the dilatational compression elastic modulus (E'). However, the experimentally accessible compression velocities are usually too high for obtaining a quasi-static compression isotherm (our experimental velocity of compression was 0.06 nm² min⁻¹ molecule⁻¹). Therefore, we performed oscillating area perturbation experiments and calculated the real and imaginary components of the complex modulus as explained in the Experimental Section. Figure 4A and B shows the E' and the dilatational viscosity η_d values, respectively, as a function of the oscillating frequency for monolayers of different DSPC/DMPC proportions and for an amplitude of 2%. When the perturbation frequency increases, the monolayers become less viscous (Figure 4B). This is expected, since if the vibrational period of the stress is large (low frequency) compared to the relaxation time of the system, then the vibrational motion of the molecules will partially degenerate into translational motion, and the resulting displacement will be translated to viscous flow. On the contrary, when a mechanical perturbation is rapidly applied to the monolayer, it responds elastically at first, just as if it was a solid body. On the other hand, the higher E' and η_d values correspond to monolayers with the higher amount of DSPC. The values obtained for E' and η_d increase for DSPC proportions above about 70 mol % and remain relatively constant at lower proportions (see Figure 3B and C).

3.3. Domain and Microbead Brownian Motion. In the two-phase coexistence region, domain Brownian motion allows the determination of the domain diffusion coefficient and consequently, the monolayer shear viscosity (η_s).[3,7,32] However, for DSPC proportions lower than 23% or pure DSPC and DMPC monolayers, a foreign probe must be added. In the latter cases, we analyzed the Brownian motion of micrometer-sized latex beads. The D values for beads (D_B) and for domains (D_D) were determined as explained in the Experimental Section. As previously observed,[7,26,33] both D_B and D_D show high data

(31) Brown, R. E.; Brockman, H. L. Using monomolecular films to characterize lipid lateral interactions. *Methods Mol. Biol.* **2007**, *398*, 41−58.
(32) Petrov, E. P.; Schwille, P. Translational diffusion in lipid membranes beyond the Saffman-Delbruck approximation. *Biophys. J.* **2008**, *94* (5), L41−L43.
(33) Sickert, M.; Rondelez, F. Shear viscosity of langmuir monolayers in the low-density limit. *Phys. Rev. Lett.* **2003**, *90* (12), 126104.
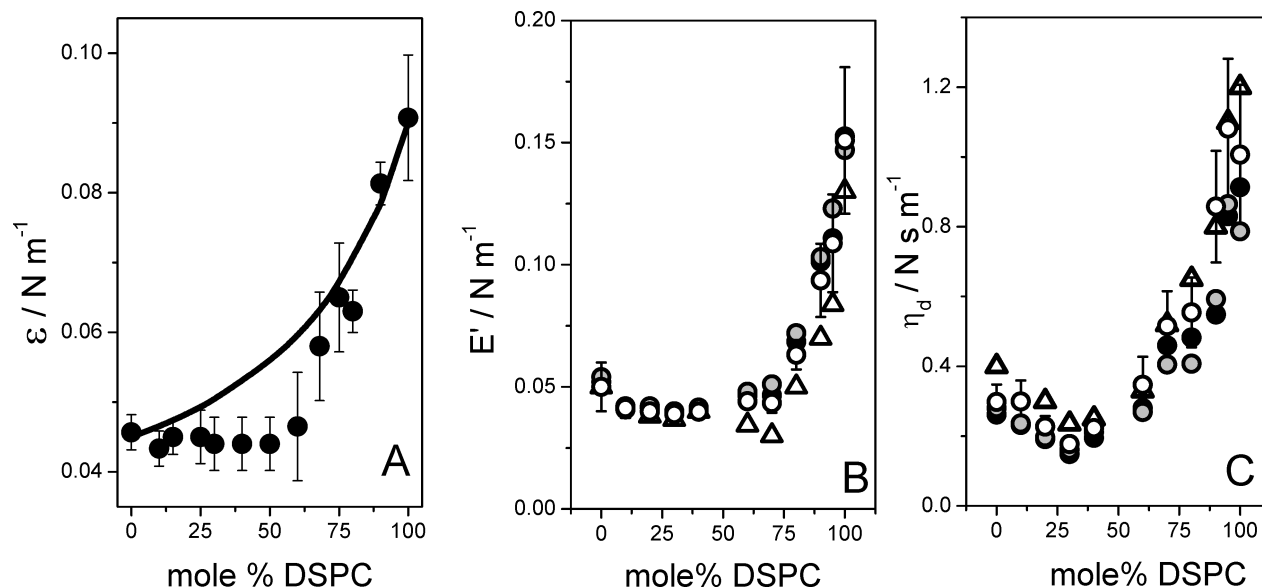
Figure 3. Monolayer compression properties as a function of the DSPC content: (A) dilatational compression modulus calculated from the compression isotherm, (B) elastic modulus of the complex compression modulus, and (C) dilatational viscosity. In (A), the compression was performed at 0.06 nm^2 min^{-1} $molecule^{-1}$. In (B) and (C), the symbols correspond to an oscillation frequency of 30 mHz and to an area oscillation amplitude of 2 (triangles), 3 (open circles), 4 (black circles), and 5% (gray circles). The error bars corresponds to oscillations with an amplitude of 4%. The other amplitudes shown result with similar data dispersion.
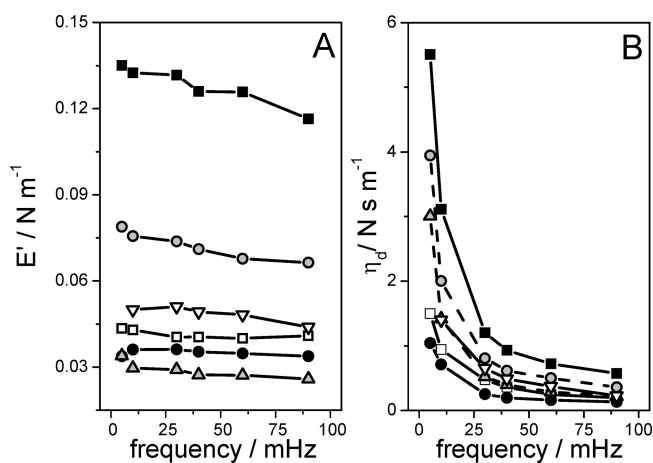

Figure 4. Elastic component of the complex compression modulus (A) and dilatational viscosity (B) as a function of the oscillation frequency for monolayers of DSPC/DMPC with different proportions of DSPC: 0 mol % (open squares), 40 mol % (black circles), 70 mol % (gray up triangles), 80 mol % (open down triangles), 90 mol % (gray circles), and 100 mol % (black squares). Area oscillation amplitude: 2%.

dispersion, specially for high D values. This is clearly shown in Figure 5, where the data histograms for different DSPC/DMPC proportions are shown. It is important to remark that the data plotted in Figure 5 were obtained from a single experiment and that independent experiments showed similar histograms. In the case of beads or domains that bear high drag forces (films with proportions of DSPC higher than 60 mol %), the histograms are sharp, while diffusion coefficients for beads and domains in a less viscous environment show a more broad data distribution (Figure 5).

In spite of the wide data dispersion, an average D value can still be calculated, since, as already mentioned, independent experiments showed similar data histograms. This can be observed in Figure 6, where the diffusion coefficients of two independent experiments for some DSPC proportion are shown (see, for example, the black dots at 40 or 50 mol % DSPC or the stars at

10 or 20 mol % DSPC); the D values for the independent experiments are the same within errors.

Figure 6 shows the diffusion coefficients determined for beads (stars), for isolated domains (gray circles), and for domains in an unperturbed array calculated from the MSD_{rel} derived from the tracking of close pairs of domains (black symbols), from pairs of domains largely separated or for a single domain, subtracting an average convection (open symbols, see Experimental Section). The image shows a representative tracking of a bead.

As observed in Figure 6, the domain diffusion coefficient decreases as the DSPC amount in the lipid mixture increases for DSPC proportions higher than 45 mol % (determined from the MSD_{rel} of close pairs of domains) or higher than 50% (determined from single domain tracking or from the MSD_{rel} of pairs of largely separated domains). On the other hand, the D_B value remains constant for DSPC/DMPC mixed monolayers in the one-phase region and for 30 mol % DSPC, and slightly decreases for monolayers with 40 mol % of DSPC (see Figure 5B). Finally, in pure DSPC monolayers, the Brownian motions of the beads are highly impeded.

The domain diffusion coefficients determined by the different methods differ for intermediate DSPC proportions. For monolayers with low domain density, domain motion is uncoupled from their closest neighbors. On the contrary, for monolayers with high domain densities, domain motion is coupled not only to their closest neighbors but to all neighbors in the array, resulting in a highly impeded motion. However, for intermediate domain densities, the diffusion coefficient depends on the data analysis and care must be taken not to underestimate the diffusion coefficient values due to coupling of the motion of close domains.

The diffusion coefficient of species in the monolayer is influenced by the monolayer shear viscosity η_s. Therefore, with a suitable mathematical model, the η_s value could be determined from the tracking of particles in the monolayer. The case of domain motion was described in detail by Hughes et al.[34] and

(34) Hughes, D.; Pailthorpe, B.; White, L. The translational and rotational drag on a cilinder moving in a membrane. *J. Fluid Mech.* **1981**, *110*, 349−372.

Stone and Ajdari,[35] and successfully employed in several reports.[3,7,32,36,37] In this work, the η_s value could be obtained from domain tracking for DSPC proportions higher than 35 mol %. For monolayers with 30 or 35 mol % DSPC, the monolayer surface viscosity is very low. Therefore, the η_s value does not influence domain movement of the micrometer-sized domains.[34] In these conditions, $D_D = k_B T / 8\eta_w R_{dom}$, where η_w and R_{dom} are the subphase viscosity and the domain radius, respectively, and the remaining parameters have their usual meaning. Figure 7A shows that there is a good agreement between the experimental and theoretical D_D values as a function of R_{dom} for monolayers with 30 mol % DSPC.

For monolayers with larger DSPC percents, the diffusion coefficient of isolated domains remains constant, indicating that the continuous phase surface viscosity is not altered by the presence of the condensed phase, as expected from the lever rule for DSPC proportions below 65 mol %.

However, domain−domain interactions hinder domain motion, and the domains sense a higher apparent surface viscosity. Using the Hughes et al. model for domain motion,[34] the apparent monolayer viscosity was calculated and the values obtained are plotted in Figure 7B (circles). As expected, the η_s values increase with the DSPC proportion. The black circles correspond to the η_s values obtained from diffusion coefficients calculated from the tracking of close pairs of domains. These values are different from those obtained from the diffusion coefficient of pairs of domains largely separated, or from the tracking of single domains (white symbols), with the latter values being the apparent viscosity sensed by the domains in the biphasic monolayer.

As already mentioned, in the composition regions where the monolayer is homogeneous, the shear viscosity has to be calculated from the bead motion. Several theoretical approaches aimed at describing the motion of particles protruding in the subphase have been reported. Sickert et al.[25] compared the diffusion coefficient of spheres inserted in a monolayer with that observed on a clean air−water interface (without the surfactant) and estimated the shear viscosity considering different mathematical approaches.[38,39] This approach could be used provided the volume of the spheres protruding in the subphase is the same at both interfaces.

The average diffusion coefficient for beads at a clean interface is $(0.38 \pm 0.26)\ \mu m^2\ s^{-1}$. For comparison, the theoretical value for a fully immersed sphere of a radius of 0.45 μm and a subphase viscosity of 0.001 N s m^{-2} is 0.47 $\mu m^2\ s^{-1}$. This value is comparable to the experimental value, taking into account the rather large dispersion of data (see Figure 5B). We conclude from the D_B values obtained that the bead is almost totally sunk in the subphase when the interface is clean. If that was also the case for lipid monolayers, the change in the bead motion of beads in the monolayer compared to that of beads in a clean interface should reflect the influence of the monolayer shear viscosity.

To decide if this was the case in our experiments, we estimated the minimum and maximum η_s values as in the work published by Sickert et al.[25] Briefly, we calculated the ratio of the diffusion coefficient value of a bead in the monolayer to that of the bead in a clean interface ($D_B/D_{clean\ interface}$); see Table 1. Several theoretical predictions of the dependence of $D_B/D_{clean\ interface}$ on the Boussinesq number ($\zeta = \eta_s / \eta_w a$, where a is the bead radius) are shown in the report of Sickert et al.[25] (Figure 4 in this paper) and allowed us to obtain a minimum and a maximum value for the surface shear viscosity in our system. These values were compared with the η_s values obtained from the domain motion. This comparison can be performed only for 40 mol % DSPC, since for monolayers with a lower DSPC proportion only an upper limit of the shear viscosity can be given from the D_D values ($\eta_s < 2 \times 10^{-10}$ N m s^{-1}), and for larger proportions the area available for the movement of beads is reduced, and therefore, the beads could be changing the mechanical properties of the monolayer. Table 1 and Figure 7B (gray triangles) show the range of values obtained for η_s. With this approach, the estimated shear viscosity values are at least 3 times larger than those calculated from the domain motion, indicating that the bead protrusion into the subphase is not similar in both interfaces.

On the other hand, Fischer et al.[39] reported a work extending the previously mentioned description of Hughes et al.[34] and Stone and Ajdari[35] for two-dimensional to three-dimensional objects. In their work, the authors gave simple analytical expressions for the drag coefficients of spheres in the limiting case of a low Boussinesq number ζ (see eqs 4.13 and 4.14 in the report by Fischer et al.[39]). Following their approach, we could determine whether the beads are floating or sunk in the subphase when immersed in the monolayer. For a monolayer composed of 40 mol % DSPC, $D_B = 0.06\ \mu m^2\ s^{-1}$ and $\eta_s = 0.4 \times 10^{-9}$ N s m^{-1} (from the D_D values), from where $\zeta = 0.9$ ($a = 0.45\ \mu m$). From these values, the friction coefficient f for the beads in this environment is $f = k_B T / D_B \eta_w a = 148$. In the approach followed by Fischer et al., the friction coefficient is expanded in a series of ζ:[39] $f = f^{(0)} + f^{(1)}\zeta + o(\zeta^2)$. Then knowing ζ and f for a given system would allow us to find the corresponding $f^{(0)}$ and $f^{(1)}$ values and the percent of the bead protruding into the subphase.

Our results for monolayers with 40 mol % DSPC indicate that the bead is mostly in the air phase, slightly touching the monolayer, in opposition to the bead position on clean subphases. In this condition, $f^{(0)} \approx 0$ and $f^{(1)} = f/\zeta$[39] ($\approx$164 for monolayers with 40% DSPC). We do not know whether the extent of protrusion of the sphere changes with the DSPC proportion in the monolayer. However, in order to have an estimation of the corresponding shear viscosity, we will assume that the beads remain in the same position relative to the plane of the interface, in all the lipid proportions analyzed. Then, with the calculated $f^{(0)}$ and $f^{(1)}$ values, we could estimate the shear viscosity for monolayers of the different DSPC/DMPC proportions. The values are plotted in Figure 7B (black triangles) and listed in Table 1. For monolayers of pure DSPC, the expansion of f in series of ζ is no longer a good approach, since ζ is large ($\zeta = 187$). Fischer et al. also proposed a simple analytical expression for cases with large ζ values (eq 4.3 in their report[39]). However, this expression requires knowing the contact angle of the liquid interface with the sphere, which is unknown under the analyzed experimental conditions. Therefore, the value of η_s for pure DSPC monolayers plotted in Figure 7B (calculated with the approach for low ζ values) is only a rough estimation of the real η_s value.

(35) Stone, H. A.; Ajdari, A. Hydrodynamics of particles embedded in a flat surfactant layer overlaying a subphase of finite depth. *J. Fluid Mech.* **1998**, *369*, 151−173.

(36) Klinger J. F.; McConnell H. M. Brownian motion and fluid mechanics of lipid monolayer domains. *J. Phys. Chem.* **1993**, *97*, 6096−6100.

(37) Steffen, P.; Heinig, P.; Wurlitzer, S.; Khattari, Z.; Fischer, Th. M. The translational and rotational drag on Langmuir monolayer domains. *J. Chem. Phys.* **2001**, *115* (2), 994−997.

(38) Danov, K.; Aust, R.; Durst, F.; Lange, U. Influence of the surface viscosity on the hydrodynamic resistance and surface diffusivity of a large brownian particle. *J. Colloid Interface Sci.* **1995**, *175*, 36−45.

(39) Fischer, Th. M.; Dhar, P.; Heinig, P. The viscous drag of spheres and filaments moving in membranes or monolayers. *J. Fluid Mech.* **2006**, *558*, 451−475.
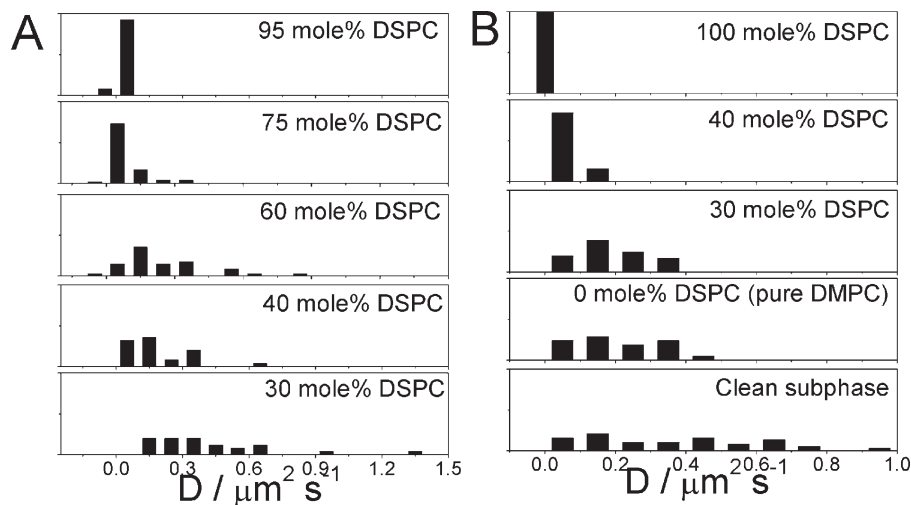
Figure 5. Histograms of the diffusion coefficient values determined for domains (A) and beads (B) in monolayers of the indicated compositions. All the *y* axes go from 0 to 1.
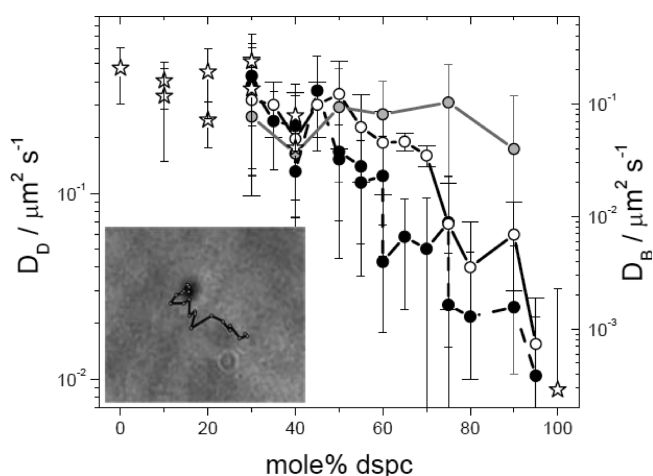

Figure 6. Diffusion coefficients of domains (circles, left scale) and beads (stars, right scale) as a function of the monolayer composition. The gray circles correspond to domains in a region of the monolayer depleted of domains ("isolated" domains, see text). The black and white circles correspond to domains in the unperturbed array of domains calculated with the MSD_{rel} of close pairs of domains (black) and with the MSD_{rel} of pairs of domains largely separated, or from the tracking of single domains (white, see text). The inset shows a representative tracking (for 20 s) of a bead in a DMPC monolayer. Image size: $30\,\mu m \times 20\,\mu m$.

In 2000, an alternative approach was reported.[40] Dimova et al. considered that the drag coefficient depends not only on η_s but also on E', η_d, and the surfactant diffusion coefficient. In their work, the coupling with the subphase liquid was neglected. For beads sunken in the subphase, the subphase viscosity should influence their motion; however, for beads floating at the interface as it seems to be our case, the subphase viscosity can probably be neglected. Therefore, we considered the applicability of the model proposed by Dimova et al. to our experimental results. According to their model, the drag force depends on the sum of $\eta_d + \eta_s$; therefore, in our case, the shear viscosity should not influence the bead motion since $\eta_d \gg \eta_s$ ($\eta_d \approx 10^{-1}\,\mathrm{N\,s\,m^{-1}}$ and $\eta_s \approx 10^{-10}\,\mathrm{N\,s\,m^{-1}}$). This implies that the bead diffusion coefficient would be

(40) Dimova, R.; Danov, K.; Pouligny, B.; Ivanov, I. B. Drag of a solid particle trapped in a thin film or at an interface: influence of surface viscosity and elasticity. *J. Colloid Interface Sci.* **2000**, *226* (1), 35–43.

similar for monolayers with similar η_d values (0–60 mol % DSPC). However, Figure 5B clearly shows that the D_B value for beads in a monolayer composed of 40 mol % DSPC is smaller (by 3 times) than the value for beads in a 0–30 mol % monolayer. This means that, in our experiments, the dilatational viscosity is not the predominant parameter influencing the bead motion.

In conclusion, the theory that better models our experimental data appears to be that proposed by Fischer et al.[39] However, the protrusion and contact angle of the spheres inserted in the monolayer should be known for a complete testing of the existing models. Besides, we cannot rule out the possibility that the bead position relative to the plane of the interface changes with the DSPC proportion in the mixture.

4. Discussion

The observation of DSPC/DMPC mixed monolayers at 10 mN m^{-1} using fluorescence and BAM microscopy shows that, on the micrometer scale, this mixture is miscible up to a proportion of about 23 mol % of DSPC. Higher proportions (over about 65 mol %) induce phase segregation and in such proportions, two phases coexist: a continuous phase with a saturating proportion of 30 mol % DSPC and micrometer-sized domains of an almost pure DSPC phase. In mixed monolayers with DSPC proportions higher than 65 mol %, either the continuous phase composition changes, becoming enriched in DSPC, or the average molecular area of the molecules in each phase changes. The percentage areas occupied by each phase reach a plateau value of about 50%.

We now define three regions in order to simplify discussion: (A) 0 mol % < DSPC ≤ 23 mol %, (B) 23 mol % < DSPC ≤ 65 mol %, and (C) 65 mol % < DSPC < 100 mol %.

A. 0 mol % < DSPC ≤ 23 mol %. In this composition region, none of the analyzed rheological properties appear to depend on the DSPC proportion and the values are similar to those observed for pure DMPC monolayers over the full range. Furthermore, the average molecular area at 10 mN m^{-1} remains constant and very similar to that of DMPC (inset in Figure 1). Our results suggest that the DSPC hydrocarbon chains become more fluidlike, increasing the number of gauche conformers and thus showing the same packing behavior as that of their analogue that is 4 carbons shorter. This could be explained considering that DSPC chains are diluted in a liquid-expanded DMPC matrix in which the restraining van der Waals interactions between the
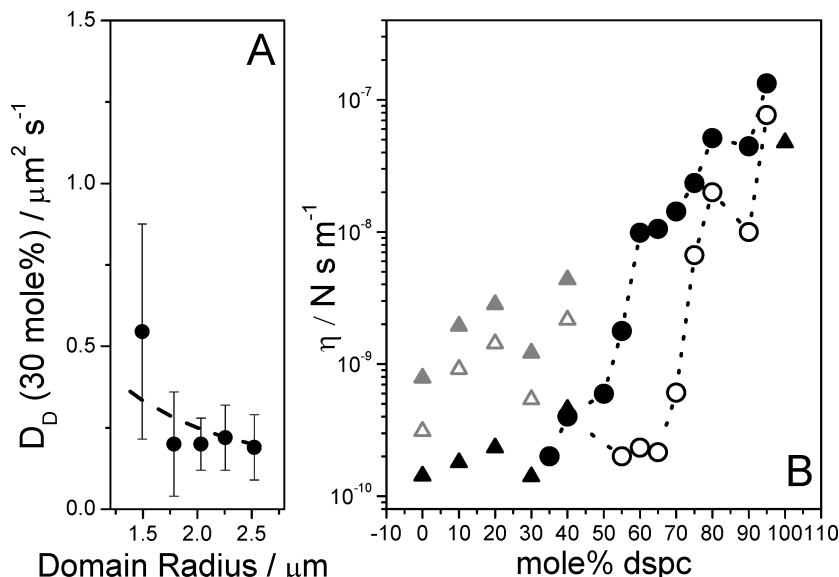
Figure 7. (A) Diffusion coefficient for domains in monolayers with 30 mol % DSPC as a function of their size. Symbols: experimental values. Line: expected theoretical curve (see text). (B) Shear viscosity for monolayers as a function of their composition calculated from the diffusion coefficient of domains following the model of Hughes et al.[34] (circles) and from the diffusion coefficient of beads following the model of Fischer et al.[39] (black triangles) or the approach proposed by Sickert et al.[25] (gray triangles). See Table 1. The white and black circles correspond to the respective D_D values shown in Figure 6.

Table 1. Diffusion Coefficient Values (D_B) for Beads in Monolayers of Different Composition[a]

DSPC mol %	D_B ($\mu m^2 s^{-1}$)	$D_B/D_{clean\ interface}$	η_s ($\times 10^{-9}$ N s m^{-1})[b]	η_s ($\times 10^{-9}$ N s m^{-1})[c]
0 (pure DMPC)	0.2 ± 0.1	0.55	0.3−0.8	0.1
10	0.16 ± 0.07	0.42	0.6−1.4	0.2
10	0.12 ± 0.09	0.31	1.2−2.5	0.2
20	0.07 ± 0.03	0.19	2.5−4.7	0.3
20	0.2 ± 0.1	0.51	0.4−0.9	0.1
30	0.24 ± 0.08	0.63	0.2−0.5	0.1
30	0.14 ± 0.07	0.36	0.9−1.9	0.2
40	0.06 ± 0.03	0.16	> 2.5	0.4 (reference)

[a] At least 40 trajectories were tracked in each independent experiment, and the diffusion coefficients obtained were averaged. For 10, 20, and 30 mol % DSPC, duplicate experiment were performed and the resulting data are presented separately. [b] D_B relative to the value in a clean interface and shear viscosity (η_s) of the monolayer calculated as in ref 25. [c] D_B relative to the value in a clean interface and shear viscosity (η_s) of the monolayer calculated as in ref 39.

longer chains become hindered when there is less than one DSPC molecule for every three DMPC molecules.

B. 23 mol % < DSPC ≤ 65 mol %. This composition region consists of a two-phase region, with the density of domains depending on the amount of DSPC in the mixture. However, its presence does not affect the compressibility of the monolayer, showing similar values to those of a pure DMPC monolayer and of the continuous phase. Over this region, the monolayer rigidity is determined by the continuous phase dilatational properties.

On the contrary, the domain diffusion coefficient stars to decrease (from 0.3×10^{-12} μm^2 s^{-1} for monolayers with 30−50 mol % DSPC, reaching 0.2×10^{-12} μm^2 s^{-1} for monolayers with 65 mol % DSPC) as the domain density increases. The domain−domain interaction (dipolar and steric repulsion) influences the domain motion, translating to a progressively more impeded Brownian motion.

C. 65 mol % < DSPC < 100 mol %. In this composition range, all the analyzed rheological properties are strongly influenced by the DSPC proportion in the mixture. The ε, E', and η_d values increase sharply, while D_D continues to decrease. The domain diffusion coefficient changes from 0.2 μm^2 s^{-1} (for 65%) to values close to the detection limit ($\approx 5 \times 10^{-3}$ μm^2 s^{-1}, which comes from following the same domain several times).

This change could be due to the slight increase of domain density (the domain area percent changes from 47% to 53%) and/or due to the change of properties in each phase (the DSPC content in the continuous phase increases and/or the average area of the molecules in each phase changes). The changes in the continuous phase properties (composition and average molecular area) could influence the motion of isolated domains. With this in mind, we followed the motion of domains in regions of the monolayer where the domain density was previously diminished using a repulsive external electrostatic field (see Experimental Section). For these "isolated" domains, the domain−domain repulsion is negligible and the continuous phase properties are expected to be the same as those in the regions of the monolayers were the domain distribution is unperturbed. We found that the D_D value for "isolated" domains is independent of the DSPC mol % over all the two-phase composition range (gray symbols in Figure 6), with an average value of 0.24 μm^2 s^{-1} and with high data dispersion, similar to the D_D value observed in monolayers with ≤30 mol % DSPC. This result indicates that the diminution in the D_D value is due to the increase of the domain density and/or to a diminution in the average molecular area of the lipids inside the domain, which would translate to an increase of the dipole density inside the domain and thus in an increased domain−domain dipolar repulsion.

In the case of the compressibility properties, we can only determine the coarse grained compression modulus. We cannot determine which factor is governing the observed property.

5. Conclusions

From the analysis of the mechanical properties of mixed DSPC/DMPC monolayers over the whole range of composition, we could establish the influence of the domain density and of each phase property on the complex compression modulus, and the diffusion coefficient. We found that the monolayer compressibility is not highly influenced by the presence of domains less compressible than the continuous phase, since monolayers with 40% of the total area occupied by domains (60 mol % DSPC) are as compressible as pure DMPC monolayers. This suggests that, for this system, domain−domain repulsion is negligible in these conditions and the continuous phase compression properties largely determine the compression properties of the system.

For high domain crowding (domain area percent > 47%), the properties of the phases in coexistence change, probably because the influence of the phase boundaries on the system free energy. In these conditions, the monolayer compressibility changes abruptly. Since the phases in coexistence are changing their individual properties in these conditions, we cannot determine whether the domain density or the properties of the phases determine the observed monolayer compressibility.

In the case of shear viscosity, as already observed for other experimental systems,[2,7] domain motion is highly dependent on the domain density. The monolayer apparent shear viscosity increases continuously with the increase of the number of domains per monolayer area and affects the domain motion, and also the motion of other particles in the monolayer (the beads in the present case). For intermediate domain densities, the motion of domains close to each other is coupled. Therefore, the determination of their Brownian motion should be performed taking this into account.

The analysis of the motion of "isolated" domains allowed us to determine whether this is a joint effect of domain crowding and changes in the continuous phase properties. We found that the motion of "isolated" domains remains constant over the full composition range where phase coexistence has been observed. Therefore, the shear viscosity of the continuous phase remains constant in this range, and the change of the apparent viscosity sensed by the domains derives from domain−domain repulsive interactions.

The influence of the domain density on the compressibility and the shear measurements is consistent because when the domain crowding is high, domains are unable to exchange nearest neighbors, becoming trapped within a cage formed by the neighbors. In these conditions, domain−domain repulsion prevails over the thermal entropy and the monolayer becomes less compressible. On the other hand, we found that the increase of the compressibility modulus at high DSPC content is related to an increase in the loss component of the compressibility modulus, which is also in agreement with the decrease of the domain Brownian movement and the increase in domain−domain interaction.

The calculation of the shear viscosity from microbead motion is not as straightforward as that from domain motion. This is because some parameters such as the percent of the bead protruding to the subphase and the contact angle of the liquid interface with the bead must be known. Experimentally, it is not easy to determine these parameters for the system under study, and we found that, at least, the protrusion of the bead is strongly dependent on the interface were the bead is inserted and it probably depends also on the manner in which it is inserted. In our experiments, the beads were premixed in the lipid solution. Other authors reported experiments using beads where the bead protrusion appears to be the same on clean and on modified interfaces.[25] In the latter report, smaller polystyrene (noncarboxy-lated) beads (diameter of 0.4 μm) were incorporated from a methanol solution to the previously formed lipid monolayer. The chemical characteristics of the bead surface, the bead size, and the way the bead is introduced to the monolayer are factors that should influence the bead wettability and therefore its motion at the interface.

However, without a numerical estimation of the shear viscosity, we can determine from bead motion whether η_s in a system is changing or remains constant. For instance, we found from the tracking of beads at the interface that the shear viscosity is not affected by the presence of increasing amounts of DSPC in homogeneous monolayers on the micrometer scale (0−23 mol % DSPC). DSPC behaves as a DMPC molecule in these conditions. On the contrary, the monolayer shear appears to depend strongly on the presence of domains, since in monolayers with a domain area percent higher that 10% (>30 mol % DSPC) the bead motion is decreased by about 3 times.